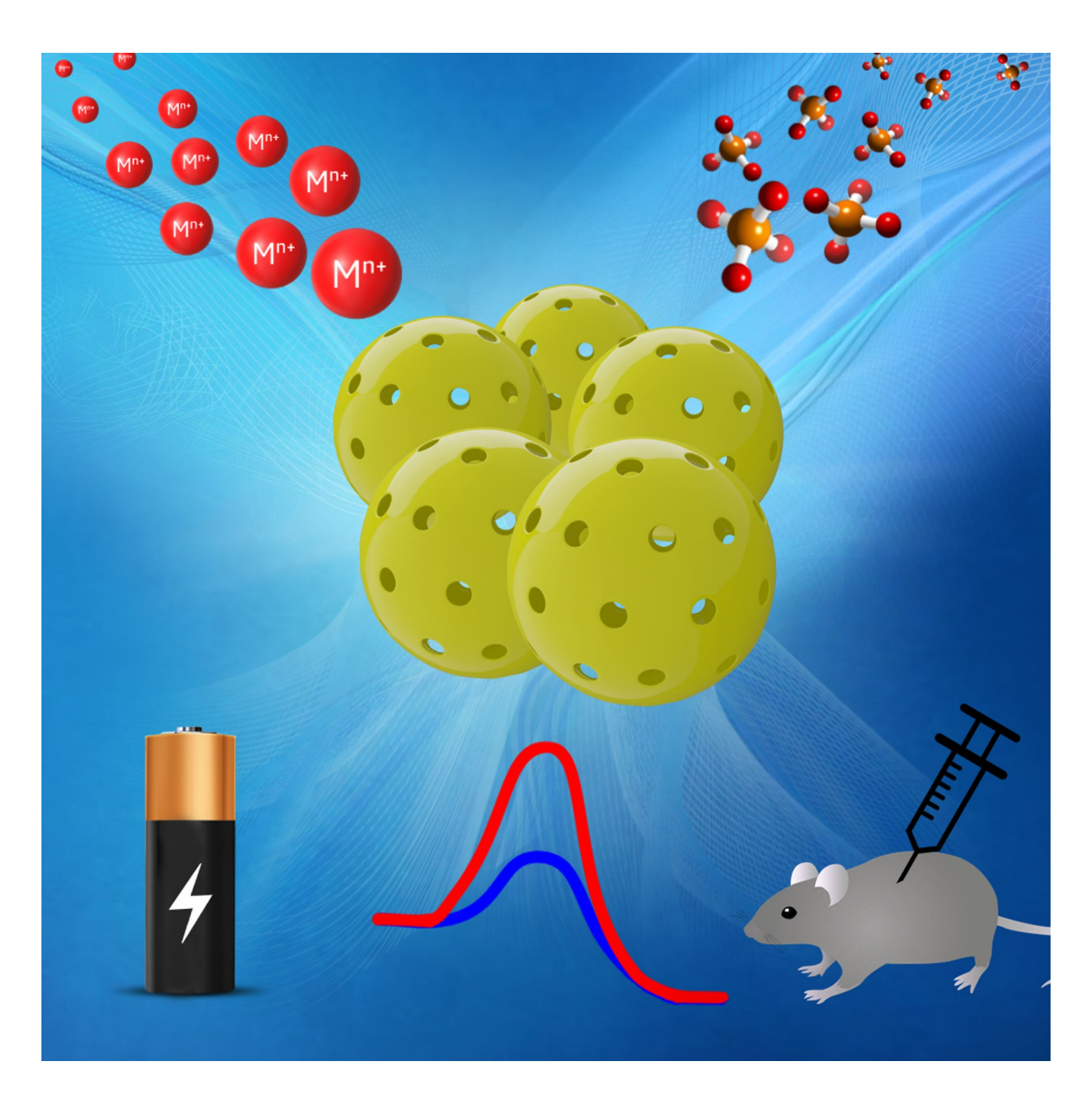
THE CHEMICAL RECORD

Hollow Structured Transition Metal Phosphates and Their Applications

Samira Munkaila $^{\scriptscriptstyle +}$, Rabin Dahal $^{\scriptscriptstyle +}$, Manzili Kokayi, Tatyana Jackson, and Bishnu Prasad Bastakoti $^{*[a]}$



Abstract: Hollow nanostructures of transition metal phosphate are of immense interest in the existing and evolving areas of technology, due to their high surface area, presence of hollow void, and easy tuning of compositions and dimensions. Emerging synthesis methods such as template-free methods, hard-templating, and soft-templating are discussed in this review. Applications of these hollow metal phosphates dominate in energy storage and conversions, with specific advantages as supercapacitor materials. Other applications, including drug delivery, water splitting, catalysis, and adsorption, are reviewed. Finally, additional perspectives on the progress of these nanostructures, and their existing challenges related to the current synthesis routes are covered. Therefore, with the strategic modifications of the unique properties of these hollow metal phosphates, broader application requirements are fulfilled.

Keywords: hollow metal phosphates, transition metal, synthesis method, catalysis, energy storage

1. Introduction

The synthesis of chemically designed inorganic metal phosphates and metal-hybrid phosphate materials embody a significant research path that has been extensively studied both in industry and academia. Various metal phosphates, particularly transition metal phosphates (TMP), possess favorable properties for catalysis, photoluminescence, and delivery. [1-6] The fine-tuning of the metal and metal bridging groups provides the infinite potential for the control and structure of the metal hybrid network in metal phosphate.^[7] The hollow form of these TMP has been synthesized in colloidal conditions resulting in the current synthetic approach of preparations with organometallic metal assembly as precursors. Likewise, due to the reasonably high specific area and abundance in surface hydroxyl groups in the metal phosphates synthesized, there has been ample use of these metal phosphates as adsorbents for dyes, radionuclide materials, and heavy metal ions. [8]

Due to the well-known photoluminescence and biocompatible properties of lanthanide phosphates, they are widely used in drug delivery and imaging. Hollow spheres of rare earth metal phosphate have been synthesized using Ostwald ripening method. The strong emission over the UV-visible range was achieved by doping other cations such as Eu³⁺, Tb³⁺, and Dy³⁺ ions. [9] Similarly, fast microwave irradiation was used to synthesize the rare-earth orthophosphate of the lanthanide family and yttrium in the mixed solution to study

[a] S. Munkaila, * R. Dahal, * M. Kokayi, T. Jackson, B. P. Bastakoti Department of Chemistry
North Carolina A&T State University
1601 E. Market St Greensboro, NC 27411
E-mail: bpbastakoti@ncat.edu

the photoluminescence with YPO4 as a representative host lattice. [10] Such properties are critical for making luminescent devices and biomedical applications. The various characteristics of these metal phosphates that enable this full range of applications include well-defined porosity, surface basicity, and tunable acidity. As with the case of vanadium phosphate, the oxidation of butane to maleic acid has been successfully commercialized, yet research is still ongoing for optimal synthetic methods and transition phases. [1,11] Another metal phosphate with a widely-known application is iron phosphate. It is recognized for its immense application in various oxidation reactions, including the selective oxidation of methane to oxygenated products and cost-effective cathode materials for high-performance lithium-ion batteries. [12] Zirconium phosphates have a wide range of applications in electrocatalytic activity due to high proton conductivity. [3,13] However, the deficiency of bulky surface properties and the domination of small interlayer spaces remain constraints for applying these metal phosphates. [14] Therefore, the synthesis of a more extended diphosphonate group could be used as a scaffold and gradually replaced by the phosphate ions to create the interlayer within the metal phosphate. [15] The UV region of solar energy makes titanium phosphate an excellent photocatalyst. However, recent research shows that the photocatalytic activity can be extended well into the visible region by introducing foreign atoms into the titanium phosphate framework. [4,16]

Hollow nanostructures are vital for many technological systems due to their large pore volume, low mass density, and high surface-to-volume ratio compared to their solid counterparts. [17-19] These characteristics make the nanomaterials advantageous for applications including energy storage, biomedicine, and catalysis. [17,20-29] The synthetic strategies for producing hollow structures are generally hard-templating, soft-templating, and template-free methods. [30]

The first part of this review article introduces the general strategies for synthesizing hollow transition metal phosphates. Secondly, the synthesis procedures are grouped into the various

^{[&}lt;sup>+</sup>] Both contributed equally.

^{© 2022} The Authors. The Chemical Record published by The Chemical Society of Japan & Wiley-VCH GmbH. This is an open access article under the terms of the Creative Commons Attribution License, which permits use, distribution and reproduction in any medium, provided the original work is properly cited.

15280961, 2022, 8, Downbaded from https://onlinelbrary.wiley.com/doi/10.1002/trc.202200084 by North Carolina A&T University, Wiley Online Library on [21/07/2023]. See the Terms and Conditions (https://onlinelibrary.wiley.com/terms-and-conditions) on Wiley Online Library for rules of use; OA articles are governed by the applicable Creative Commons. License

metal phosphates based on their applications and functions in multiple fields. Lastly, more viewpoints are provided on the issues around the synthesis methods with advanced novel strategies to explore the functionalization of these hollow metal phosphates.

2. Synthesis Strategies for Hollow TMP

Despite substantial scientific interest, the synthesis of the controlled hollow structure of transition-metal phosphates has encountered many challenges. The rapid precipitation reaction between metal ions (Mⁿ⁺) and phosphate anions (PO₄³⁻) often leads to irregular or bulk structures in the solution. A robust chelating agent or structure-directing agent is required to control the over crystal growth of metal phosphates. Micronsized nickel phosphate was synthesized using complexing molecules ethylenediamine tetra(methylene phosphonic acid) molecules. Hard templates such as silica and carbon were used to synthesize hollow structures. Ordered mesoporous tin phosphate was synthesized via nanocasting method using SBA-15 silica and CMK-3 carbon as hard templates. The mesoporous structure showed better thermal stability than

when synthesized from a conventional hydrothermal method. [32] Researchers have consistently struggled to find the appropriate dimension of template, functionalization of template, and removal of the template to get hollow structures. There have been no simple ways to prepare sub-50 nm hollow nanospheres of transition metal phosphates. Bastakoti et al. reported the single micelle template method to synthesize the sub-50 nm hollow nanospheres of metal phosphate/ carbonate. [33-35] The strong binding of metal sources and polymeric micelles leads to fabricating hollow nanospheres with controllable sizes. The polymers are designed in such a way that the metal sources are driven to interact with the specific domain of the polymer. [36-38] The molecularly dissolved polymer chains in tetrahydrofuran undergo self-assembly after adding phosphoric acid. The spherical micelles are used as templates to fabricate hollow nanospheres. The micelles have a positive surface area due to the presence of the pyridine group which interacts with positively charged metal sources through a negatively charged phosphate ions bridge. After removing the polymer template via calcination or solvent extraction, the hollow nanospheres of nickel phosphate were obtained (Figure 1).^[33]



Samira Munkaila earned her master's degree under Dr. Bishnu P. Bastakoti at North Carolina A&T state university, where she studied block copolymer-assisted synthesis of porous inorganic metal oxides and phosphates. She earned her B.Sc. in chemistry at the University of Cape Coast, Ghana in 2017. She is currently a doctoral candidate at the Molecular Design Institute, New York University.



Rabin Dahal earned his master's degree from Tribhuvan University, Nepal in 2016. He is currently a doctoral candidate at North Carolina A&T State University. He is studying the controlled synthesis of porous metal for CO₂ reduction.



Manzili is a graduating senior of an ACS certified Bachelor's of Chemistry. With a passion for green chemistry, she has focused on energy generation and storage in sustainability. She is working with Dr. Bastakoti on the project synthesis of porous NiO/C electrodes for supercapacitor.



Tatyana Jackson earned her B.S in Chemistry from Savannah State University in 2021. She is currently enrolled in the M.S in Chemistry program at North Carolina A&T State University. Where she works under Dr. Bastakoti studying oscillating chemical reactions which are used to synthesize block copolymers that are formed into porous N-doped carbon materials.



Dr. Bastakoti pursued a Ph.D. from Saga University, Japan as a Monbukagakusho scholar. Following this, he joined the National Institute for Materials Science as a JSPS Fellow. He has previously worked at the University of Sydney and Harvard University before starting his independent career at North Carolina A&T State University. He is exploring a broad design challenge to control the multiple structural properties such as porosity, crystallinity, and dimension of porous inorganic nanomaterials. He is particularly interested in using highly porous nanostructured materials in catalysis, energy conversion, and sensing.

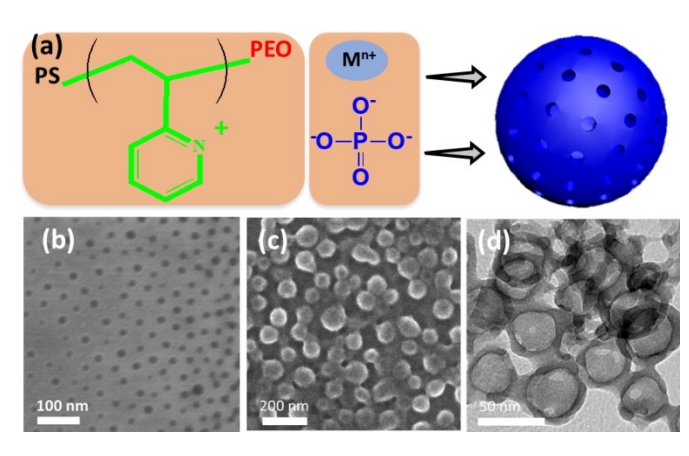


Figure 1. (a) Single micelles templating method to synthesize hollow nickel phosphate. SEM images of (a) polymeric micelles, (b) polymer- nickel phosphate composites, and (d) TEM image of hollow nickel phosphates. Reprinted with permission. [33] Copyright 2019 Elsevier Ltd.—

Zhang *et al.* reported the template-free method for the synthesis of vanadium phosphate with controlled layers. They were prepared by self-assembly of vanadyl sulfate and phytic acid. Phytic acid is a chelating agent, avoids unnecessary aggregation, and is a carbon source in hydrothermal synthesis. The x-ray photoelectron spectroscopy data clearly shows that the nanosheet has much higher V^{4+} ions than V^{5+} ions. The presence of more V^{4+} ions increases the number of electrochemical accessible surface sites. The introduction of V^{4+} ions into vanadium phosphate increases the number of defects and oxygen vacancies. [39]

The self-templating method involves the chemical integration of the model materials into the shells of the nanomaterial after template preparation. Then, there is a chemical transformation of the templates into hollow nanostructures. The templates used for this synthesis approach provide space for creating inner voids and materials to form outer shells. The self-templating method comprises a relatively simple procedure with high reproducibility and economic feasibility than the other templating methods. The challenge of using the templating method arises from the size limitation of the hollow nanoparticles and post-treatment of templates. On the other hand, the post-treatment of these nanomaterials during template removal may cause structural deformation and the introduction of a varying degree of impurities. [40] Colloidal hollow transition metal phosphates were synthesized by manipulating the reactions' primary stoichiometric ratios and pH values of the reaction. The amorphous colloidal spheres possess a range of properties resulting from the arrangement of the d-orbital electrons in these transition metals. These colloidal spheres could crystalize upon annealing in a wellcontrolled process resulting in a preserved size and morphology. [41] Commonly used methods to synthesize hollow metal phosphates nanostructure and their applications are listed in Table 1.

2.1. Hollow Iron Phosphates

Iron phosphates of various morphologies have been synthesized due to their tremendous potential and economic benefits in electrocatalysis, energy storage devices, and drug delivery. [44,59] An oil-phase synthesis method was used to produce hollow iron phosphates with nanotube morphology. The synthesized iron phosphate nanotubes were amorphous and with remarkably high surface area, therefore, employed in lithium-ion battery for energy storage devices. [44] In another study, hollow iron phosphates were synthesized by a water-in-oil microemulsion system. This system utilized the aqueous core of the reverse micelles, which were used to encapsulate the hydrophilic dye, thereby showing non-toxicity, and was easily absorbed by cells. Therefore, this hollow material offers an efficient carrier for drug delivery in biological applications and magnetic imaging. [33] Water splitting is another application where hollow iron phosphates are highly utilized due to their large surface area and potentially active catalytic sites. Hollow iron phosphates were synthesized from iron phosphide nanotubes by a template-free synthesis route involving a simple hydrothermal synthesis of iron-oxy-hydroxide as precursors. [59] Duan et al. synthesized the core-shell hollow spheres of FePO₄ using polystyrene (PS) beads as a template. It was theorized that changing the precursor ratio would produce the hollow spheres with controllable shell thickness. PS beads were used as a reaction site for the growth of FePO₄. The selective mineralization of FePO4 took place around the uniformly distributed PS beads. The removal of PS in calcination led to the formation of the hollow spheres of FePO₄ Figure 2 shows the TEM image of hollow nanospheres. The elemental mapping and X-ray photoelectron spectroscopy analysis confirmed the existence of Fe, P, and O. Interestingly the crystallinity was induced when the calcination temperatures increased from 500 °C to 800 °C. However, the high-temperature calcination sintered the particles. [60]

2.2. Hollow Nickel/Cobalt Phosphates

Xiao *et al.* Synthesized a non-spherical hollow nickel phosphate with a cobalt framework, possessing unique anisotropic properties and regulated morphology for catalysis, energy storage, and conversion. These hollow Co–Ni phosphate nanocages were prepared by shell-coating and controllable etching process by employing the ZIF-67 metal-organic frameworks (MOFs) as a template leading to a high specific capacitance, energy density, and excellent cycling stability. [47] Another non-spherical morphology is a new approach of Ni-MOF-derived hollow porous nickel phosphate synthesized by a ligand-

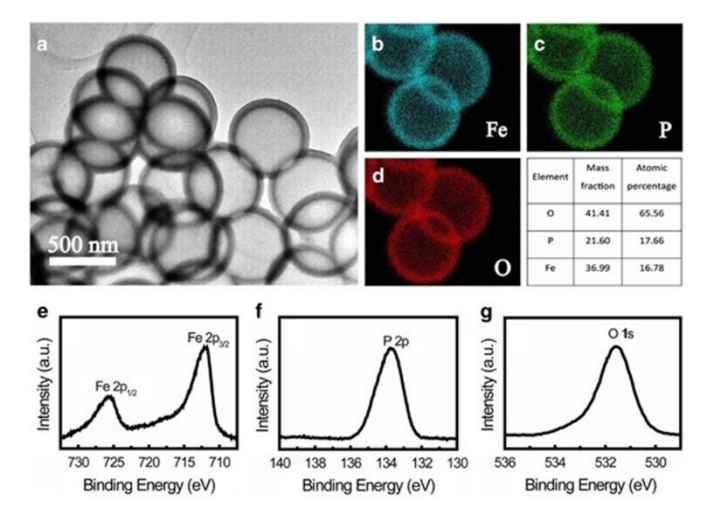


Figure 2. (a) TEM images (b—d) elemental mappings and (e–g) XPS spectra of FePO_4 hollow spheres. $^{\rm [60]}$

replacement mechanism. These 3D nanorods were prepared by a solvothermal process involving substituting ligands from the MOF with phosphoric ions. The hybrid structure depicts excellent electrode materials in applications for electrochemical supercapacitors.^[49]

More recently, hollow nickel phosphides were synthesized by Zhang and the team for similar applications in energy storage and conversion by employing metal-formate frameworks. These frameworks were achieved by the sacrificial template method, which eventually produced structure-tunable hollow nickel-cobalt microtubes. The stability of these microtubes was a result of the synergistic effect between Co and Ni ions, which provided a high specific capacitance and better electrochemical activity to the nanomaterial. [61] In another study, the sol-gel method was employed in the synthesis of hollow nickel phosphate nanotubes, which were used in catalytic applications. These NiPO₄ hollow nanotubes had a pore volume of 0.46 cm³ g⁻¹ with an exceptionally average length of approximately 600 nm. [48] Cobalt phosphates are widely known for their high oxidation ability in applications for oxygen evolution reactions, heterogeneous catalysis, ion exchangers, and positive electrodes for rechargeable ion batteries. [62,63] The synthesis of hollow cobalt phosphates has increased material utilization and improved chemical kinetics and structural sturdiness for better cycling performance. Nonspherical hollow cobalt phosphate was synthesized by Xiao et al. Using metal-organic frameworks (ZIF-67) as a template and nickel phosphate for a synergistic effect, a controlled size, phase, and morphology. [47] This method of synthesis produced hollow cobalt phosphate nanocages from ultrathin nanosheets with energy storage applications. Similarly, hollow cobalt phosphate was synthesized from cobalt phosphonates, which

shows a peculiar performance in electrolysis for oxygen evolution in alkaline conditions. The ultra-small nanoparticles of metal phosphate were decorated on the amorphous hollow carbon structure. ZIF-8@ZIF-67 core-shell structure was prepared via seed epitaxial growth. NH₄H₂PO₄ was mixed with ZIF-8@ZIF-67 and annealed at 600 °C in argon condition (Figure 3). Co and Zn phosphate incorporated in the hollow carbon structures were used as cathode materials in the Li-ion battery. $^{[64]}$

2.3. Hollow Vanadium Phosphates

Vanadium phosphates have been used for catalytic applications due to their favorable reactions, especially in surface chemistry. These functional phosphate materials have earned several benefits in electronic, energy storage, and catalytic applications resulting from the different polymorphs demonstrated by the phosphate compound. As reported by Dupre *et al.*, these polymorphs include two orthorhombic, one monoclinic, and four tetragonal structures with different energy configurations and varying synthesis routes. The composites of vanadium phosphate and iron phosphate were synthesized from yeast cells as a template. Yeast is a unicellular fungus with spherical or elliptical morphology. The protein and polysaccharides on the cell wall interact with metal ions or ionic groups to promote biomineralization. [68]

Kanta *et al.*, synthesized the carbon-coat-Na₃V₂(PO₄)₃ using a microwave-assisted sol-gel process where NaH₂PO₄·2H₂O, NH₄VO₃, and citric acid were used in the ratio of 3:2:2 to form a gel which was used as an electrode material in a sodium-ion battery. [69] Nanocomposite particles of Li₃V₂(PO₄)₃/CNT were synthesized by spray drying process followed by calcination at a high temperature. The aerosol droplets of the precursor were produced by using nitrogen carrier gas as a dispersion which passed through an atomizer. [70] SP^2 co-ordinated carbon coating mesoporous Na₃V₂(PO₄)₃

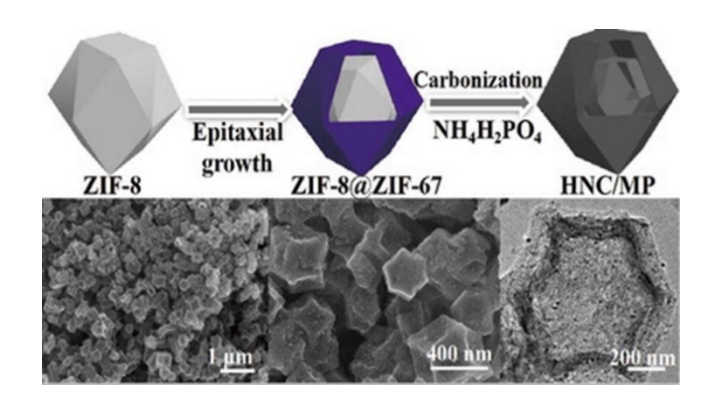


Figure 3. Synthesis of hollow Zn–Co phosphate/C nanocage with their electron microscopy images. Reprinted with permission. ^[64] Copyright 2020 Chemical Society of Japan

nanoparticles were synthesized using ascorbic acid where the acid acts as both carbon supplier and reducing agent. The sample was calcined at 750 °C in an argon atmosphere. The carbon nanotube protected vanadium phosphate-incorporated carbon nanofibers (CNTs@VPO@CNF) were synthesized by electrospinning process. In this process, Polyacrylonitrile and ammonium metavanadate (in the ratio of 4:1) were mixed, stirred, and electro-spined. The mixture was carbonized at different temperatures under a nitrogen atmosphere to obtain nanofibers. [72]

2.4. Zirconium Phosphates

In earlier years, Clearfield and Smith collectively studied the crystal structure of α- zirconium bis (monohydrogen orthomonohydrate,^[73] subsequently, phosphate) phosphate has been studied expansively in recent years due to facile synthesis, low cost, prominent stability, and vast applications including catalysis [50] and targeted ions removal. [74] More recently, a facile hydrothermal conversion method was employed in the synthesis of gadolinium phosphate hollow spheres, which increases the crystallinity of the nanomaterial upon annealing. The hollow spheres were further doped with other lanthanides increasing emission intensities. [52,53] A solvothermal method was employed to synthesize zirconium phosphate using zirconyl chloride octahydrate as a precursor and phosphoric acid maintaining the pH below 2. The solution was stirred for 12 hours followed by washing with ethanol and dried at 120 °C in an air oven overnight. Finally, the sample was calcined at 1083 K for 12 hours. [75] In another study, the zirconium phosphate microporous monolith was synthesized by the sol-gel method. The metal source was dissolved in 1 M HCl and glycerol followed by the addition of polyethylene oxide and polyacrylamide. The whole mixture was stirred and cooled to 0°C in an ice bath where the 0.41 ml of phosphoric acid at a temperature of 0 °C was added and stirred to obtain the wet gel. The gel was dried at 60°C for three days followed by calcination at different temperatures. [76] Alkoxides precursors of zirconium were used to synthesize the nanostructured porous zirconium phosphate. The zirconium n-propoxide was dissolved in orthophosphoric acid (0.1 mol/L) in the presence or absence of surfactants. The solution was divided into two parts where one part is subjected to auto-clave heating at 80°C and another part was directly dried at 60 °C to obtain different solid particles for comparison of thermal stability.[77]

2.5. Manganese Phosphates

Manganese phosphate nanospheres were synthesized using two-phase colloidal synthesis. Manganese nitrate reacts with phosphoric acid in the presence of oleylamine and octadecene

at 180 °C. The amorphous hollow nanospheres of manganese phosphate and iron-manganese phosphate possess high electrochemical surface and conductivity. The hollow manganese phosphate was synthesized using a template-free method (Figure 4).^[79] A hollow nanosphere of amorphous iron doped manganese phosphate (Fe-Mn:P) was synthesized using a two-step solvothermal method where amorphous manganese phosphate was produced at first which further reacts with iron nitrate at 180°C for 2 hours to form a hollow nanosphere. [78] The hollow nanocubes of MnCoP were synthesized by hard acid soft base principles where cuprous oxide, cobalt chloride, and manganese chloride were used followed by the phosphorization to get hollow nanocubes. [80] Ni-Mn(PO₄)₂ composite was prepared by manganese chloride and nickel chloride under probe sonication mixing with Na₂HPO₄ dropwise. Finally, the composite was calcined at 400 °C for 4 hours. The SEM image composite showed the formation of nanoflakes. [81] The Na₃Fe₂. _vMn_v(PO₄)(P₂O₇) mixed phosphate was prepared using a spray-drying method. The solution was further heated at 550 °C for 10 hours under argon.

3. Applications of Hollow Metal Phosphates

Transition metal phosphates are generally synthesized in various forms to augment intended applications. The characteristics of this class of phosphates include excellent chemical stability, mechanical flexibility, superior conductivity, high surface area, and charge transport, which in turn promotes electrochemical and diffusion applications. [82,83] Several factors influence the properties of the manufactured nanomaterial based on the synthesis strategy employed. The structure-directing strategy of creating hollow phosphates is influenced by the concentration of surfactants, choice of surfactants, inorganic metal and phosphate precursors, the formation of surfactant micelle, and removal of the template. [84] TMPs have shown a promising prospect as valuable materials for anticancer drug delivery amongst other bioapplications. [3,74,85]

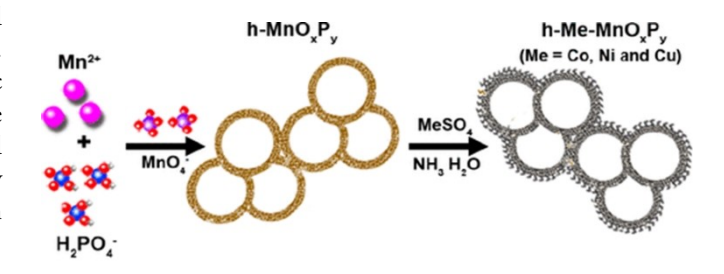


Figure 4. Self-templating synthesis of manganese phosphate hollow nanospheres. Reprinted with permission. ^[79] Copyright 2018 American Chemical Society.

Prospective applications for some lanthanide phosphates have been exploited in white light-emitting diodes, optoelectronic devices, and field emission displays. This is usually resulting from the structurally stable half-filled 4f orbitals. Deter applications of this hollow GdPO₄ include reliable bioimaging, drug delivery, and drug release system resulting from the characteristic emissions from their transition states. Hollow calcium carbonates have been widely applied as biomaterials for tissue engineering, imaging agents, and drug delivery but in recent years, the use of hollow calcium phosphates for complex bioengineering and biocompatible materials has received substantial recognition. This application is because of the nanoscale size and osteogenic cell delivery system of the hollow microspheres.

3.1. Energy Storage Devices

Zhao et. al synthesized iron phosphate nanospheres using a solvent extraction method, for possible use in energy storage. By combining PC-884 with N1923 for use in separate extractions of Fe3+ (metal source) and H3PO4 (phosphate source) and then combining the loaded phases, they were able to form FePO₄. [86] It was found to have favorable electrochemical properties, with a 40 cycle capacity retention and 100% coulombic efficiency. Interestingly, polarization had an inverse relationship to cycling, meaning the interaction between charge and discharge increased over time. It also displayed good reversibility, being able to cycle up to 80 mAh g⁻¹ multiple times. Lithium iron phosphates have been synthesized many times, with more recent studies looking into ways to make them more sustainable. Wang et al. recycled a mixture of LiFePO4/C and acetylene black. They used a physical separation based on density and regenerated the products for use in lithium iron phosphate batteries. It was found to have good electrochemical performance, with a 92.6% retention after 1000 cycles. [87] Sodium-ion batteries have been theorized to be a substitute for lithium-ion batteries. In one study, researchers were able to synthesize olivine NaFePO₄/C from LiFePO₄/C using an aqueous electrochemical displacement method. It was found to have good capacity retention, at 90% after 240 cycles and a rated capacity of 46 mAh g⁻¹. [88] Furthermore, NaTi₂(PO₄)₃ (i.e., NTP) has been applied in various energy storage systems. This includes sodium-ion batteries (i.e., SIBs), non-aqueous batteries, and aqueous batteries. NTPs act as anodes in SIBs, and have been shown to display good electrochemical properties. Nonaqueous batteries can rely on the sodiation of NTP from NaTi₂(PO₄)₃ to Na₃Ti₂(PO₄)₃, and many researchers are working to improve its electrochemical performance due to its low conductivity. Aqueous rechargeable batteries have been critiqued for their high cost, toxicity, and flammability. Naion full cell batteries were introduced as a solution to these

issues, then found to have good electrochemical properties that were better, in some ways, than non-aqueous and Li-ion secondary batteries.^[89]

Sharmilla et al. synthesized a multi-wall carbon nanotube coated nickel manganese phosphate electrode using a hydrothermal method. They found that it had good electrochemical properties, with a specific capacity of 812 Fg⁻¹, and 93% capacity retention at 5000 cycles. [90] A sonochemical method was employed in synthesizing nickel manganese phosphate. Its specific capacity was 678 Cg^{-1} at 0.4 Ag^{-1} and a 99.2% stability after 5000 cycles. [81] It was concluded that the capacitive and diffusive mechanism improved the storage capabilities of the supercapacitor. Flexible devices were synthesized using amorphous nickel pyrophosphate microstructures. Its specific capacity was 145.8 mAh g⁻¹, 105.0 Fg⁻¹, and a retention rate of 90.5 % after 6000 cycles. It also could bend between 0 °C to 180 °C. They concluded that the energy efficiency and device performance could use improvement. [91] Nickel-cobalt phosphate was used to attempt a flexible battery. This was accomplished by creating thin, two-dimensional nanosheets of the material with an aqueous/ solid-state electrolyte. Bing et al., used a one-step hydrothermal method and obtained a 1132.5 Fg⁻¹ specific capacitance, 32.5 Wh kg⁻¹ energy density. They concluded that the device was durable in a range of temperatures and would be worthy of further research in energy storage. [92] Separately, ammonium nickel-cobalt phosphate was synthesized using a two-step hydrothermal method. Wang, et. al., focused on using diffusion-controlled materials without the usual issue of depressed power density. They reported a novel core-shell composed of (NH₄)(Ni, Co)PO₆·0.67 H₂O nanosheets @ single-crystal macroplatelets (NH₄)(Ni, Co)PO₆·0.67 H₂O (NCoNiP@NCoNiP). The device was found to have good electrochemical properties and adequate power density. [93] Also, cobalt phosphate was synthesized by Iqbal, et. al., using a sonochemical and hydrothermal method. Its specific capacity was 221.4 Fg⁻¹, power density was 6800 Wh kg⁻¹, energy density was 34.75 Wh kg⁻¹, and retention was 87.2% after 10,000 cycles. They concluded that the sonochemical approach, though novel, proved beneficial in controlling structural properties. [94] Bimetallic hollow phosphate was synthesized and used for high supercapacitor performance. The coating and controllable etching of the process leads to the formation of a hollow structure (Figure 5). The hollow Co/Ni phosphate nanocages exhibit a high specific capacitance of 1616 F g⁻¹ with 33.29 Wh kg⁻¹ energy density at 0.15 kW kg⁻¹ power density.[47]

3.2. Bio-Applications of Metal Phosphates

Phosphorus plays a vital role in our body: (1)It is one of the most fundamental components of nucleic acids, which make

and-conditions) on Wiley Online Library for rules of use; OA articles are governed by the applicable Creative Commons License

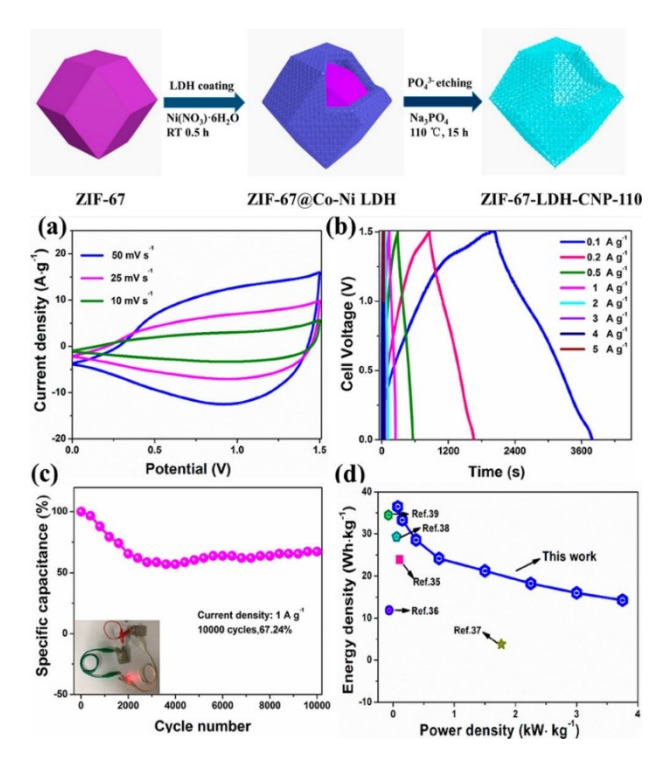


Figure 5. Synthesis of Ni–Co phosphate nanocages and their application as electrode materials in supercapacitors. Reprinted with permission. [47] Copyright 2019 American Chemical Society.

up genetic contents; (2) it is an essential component of body fluid; and (3) it is used to produce proteins, teeth, and bone. Almost all of the critical advances in the domains of biology and biochemistry in the new century are intimately tied to compounds containing phosphorus, opening up a very appealing universe for phosphorus compounds' use. Many phosphorus-based inorganic nanomaterials have been developed and widely used in biomedical applications due to the fast development of nanotechnology. [95–99] Inorganic metal phosphates have numerous biomedical applications including drug delivery and magnetic resonance imaging, alpha therapy, colorectal cancer studies, and enhanced cytocompatibility and osteogenic efficiency.

Transition metal phosphate hollow nanospheres with large proportions of void space have gotten a lot of interest in drug delivery and medical imaging markers. Hollow spheres have many unique and superior properties to accommodate a large amount of payloads and improve permeability. Calcium phosphate possesses distinct biocompatibility with the ability to attain a tailorable bio-absorbability and bioactivity. Various trace elements are commonly found in biological systems' hydroxyapatite (HA) materials. Zinc is a trace element that is required forhuman health. It is the second most prevalent transition metal in organisms after iron. It is also thought to have antioxidant effects and suitable for immunological

system. The hollow hydroxy zinc phosphate nanospheres have a high drug loading content of 16.28±0.44 % wt. percent at room temperature. [100] To back up this claim, TEM with EDX (energy-dispersive X-ray spectroscopy) was used to analyze the shape and elements of drug-loaded hydroxy zinc phosphate nanospheres (HZnPNSs). The findings proved that the medication had been put within the hollow spheres. The therapeutic impact of medicine is directly linked to the drug release behavior in the body. The usual pH of blood for human survival is around 7.4, although the environment of cells' endosomes and lysosomes is more acidic. HA degrades more slowly than hydroxyl zinc apatites. At mild temperatures of no more than 25°C, HZnPNSs were synthesized using a bio-friendly and template-free technique. HZnPNSs have efficient protein adsorption and a high drug loading capacity. After oral delivery of lanthanum carbonate tablets to patients, lanthanum can inhibit phosphate absorption by generating lanthanum phosphate complexes. Hollow YPO₄ with Tb³⁺ and Eu³⁺ dopant shows orange and green emissions under UV excitation and also possess sustainable drug release with excellent biocompatibility. [101] The chitosan-coated siRNAloaded lanthanum phosphate nanoparticles were prepared to improve cancer treatment based on the pH-responsive release of payloads. The excessive growth of lanthanum phosphate was controlled by using polysaccharides and chitosan. As a result, the lanthanum-based siRNA delivery system could be a promising and effective therapy option for colorectal tumors. [102,103] Figure 6 shows the preparation of siRNA-loaded lanthanum nanoparticles where the decrease in pH value increases the particles' size. Similarly, the release of siRNA from the nanoparticles was higher at lower pH (4.5) as compared with higher pH (7.4). [103]

Magnetic resonance imaging (MRI) is a dynamic imaging method that has offered excellent spatial resolution and outstanding anatomical features of soft tissues without the use of radioisotopes in both clinical and research applications. The

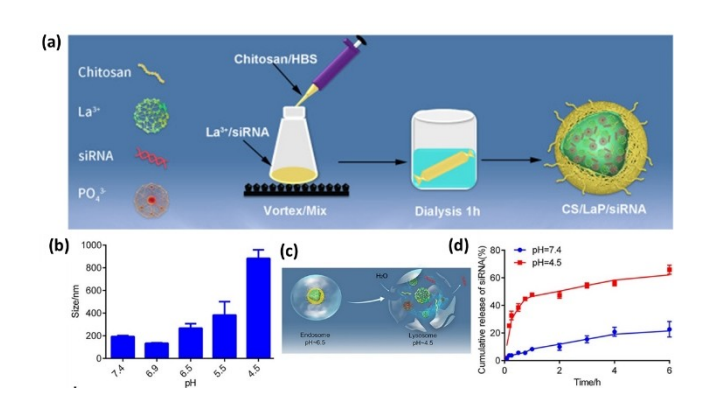


Figure 6. Using hollow lanthanum phosphate for delivery of siRNA. Reprinted with permission. [103] Copyright 2020 Elsevier Ltd.

mostly used magnetic NPs such as MFe_2O_4 (M=Fe, Co, Mn) in MRI produce a dark signal that can be confused with bleeding, calcification, or metal deposits, potentially leading to misdiagnosis. One of the most complex challenges in tumor detection and treatment is identifying tumors from normal cellular tissue and releasing medications selectively at the target place. By utilizing the pH differential between the intracellular and external environments, MRI-based cell tracking for diagnosis can be accomplished. Hollow manganese phosphate nanoparticles (HMP NPS) are amorphous and the release of Mn^{2+} ions can be controlled by tuningthe pH of the solution. The functionalized HMP NPs can be used as a multifunctional probe for MRI-guided selective diagnostics and medication delivery. [104]

Targeted alpha treatment (TAT) can kill tumor cells while causing minimal collateral damage to healthy tissue. The resistance to radiation damage of lanthanide phosphates makes them promising candidates in radioimmunotherapy (RIT), TAT, and imaging applications. The core-shell structure of LaPO₄ nanoparticles containing either ²²³Ra or ²²⁵Ra was synthesized to study the ability to disintegrate into daughter nuclei in vitro. It is found that the retention of Ra parents and related daughters within core and core-shell is substantially higher in LaPO₄. As a result, the core and core-shell LaPO₄ NPs could be used as radionuclide carriers in RIT, TAT, and medical diagnostic imaging. ^[105]

3.3. Catalysis and Adsorbent

Vanadium phosphate-zirconium phosphate (VP-ZrP) nanocomposites were used for gas phase dehydration of glycol to acrolein. Those catalysts were synthesized by the solid-solid wetting method. The surface area analyzer revealed that the total surface area and the pore size of zirconium phosphate decrease on loading VP from 5–30% by wt. An active phase was observed in highly dispersed form when an increase in VP loading above 20% by wt. Temperature-programmed reduction (TPR) showed the greater reducibility of species containing lower VP loading. The selectivity of acrolein by VP supported on ZrP decreased at first as compared to pure VP. However, later, it goes on increasing when % by wt. of VP increased from 5–20%. [106]

Guaiacol is widely used in dental pulp sedation and has the special property of inducing cell proliferation and scavenger of reactive oxygen species. Conventionally it was synthesized from toxic, expensive agents. Transition metal (M=La, Ce, Mg, Al, Zn) phosphates were successfully used to synthesize guaiacol via a more economical and environmentally friendly route. The alkylation of O-methylation of catechol (1,2-dihydroxy benzene) with methanol gives guaiacol. Among the used metal phosphates, cerium phosphate showed the highest catechol conversion (80.3%). The catalytic performance of

cerium phosphate occurs in two cycles. At first, the performance goes on decreasing from 71.7% to 43.3% which gets stable after 72 hours and finally increases again and reached up to 66.5% due to regeneration of catalyst for the conversion of catechol. In the second cycle, the performance of regenerated cerium phosphate catalyst decreases from 66.5% to 37.8% after a certain time of the stream. However, the selectivity of guaiacol was less after the regeneration of cerium phosphate than initially. Moreover, the catalytic activity of transitional metal phosphate catalyst can also be studied by the acidity of the catalyst. [107] Iron doped manganese phosphate(Fe-Mn:P) synthesized through the hydrothermal method was used as a heterogeneous electrocatalyst for electrocatalytic oxygen evolution reaction (OER) (Figure 7). The efficiency was compared with nickel foam, IrO2 (commercially available), and manganese phosphate in an alkaline solution. The greater activity and higher stability of a-Fe-Mn:P catalyst towards OER in alkaline solution was justified by the lowest overpotential of 252 mV at 10 mA cm⁻², lowest Tafel slope value of 52 mV dec⁻¹ and astonishing catalytic stability upto 20 hours and finally maintaining 93% of the initial value of current density.[78]

Molybdenum phosphate (MoP) has metal ions in various oxidation states, $\mathrm{Mo^{3+}}$, $\mathrm{Mo^{5+}}$, $\mathrm{Mo^{6+}}$ ions, and in some cases their mixture. Such redox properties make them ideal catalysts for partial or complete oxidation of hydrocarbons. Vanadium-promoted molybdenum phosphate was used to study the partial oxidation of methanol to formaldehyde. The increased concentration of vanadium (10 % and 20 %) showed a separate VP phase with characteristic platelet morphology. The bulk reducibility studied by TPR analysis showed a substantialin-crease in $\mathrm{H_2}$ consumption for both $\mathrm{MoP-V10}$ and $\mathrm{MoP-V20}$ in comparison with MoP and MoP containing less concentration of vanadium. The higher vanadium concentration in MoP enhanced the selective activity as compared to unprompted MoP .

Nitrogen-doped metal phosphate was synthesized by controlled calcination of synthesized metal ammonium phosphate by a simple method. The metal-like (M=Co, Mn, Nior Cu) were used to synthesize metal ammonium phosphate and nitrogen-doped metal phosphate. Field emission scanning electron microscopy analyzed the morphology of the synthesized materials and revealed the flower-like morphologies in both ammonium and nitrogen-doped cobalt phosphate(N-CoP). The transmission electron microscopy images showed the sheet-like structure constituting pore distribution. The pore diameters are of 3-10 nm without the ordered pore structure. However, in the case of N-MnP, the pores are at the surface, and they are uniform. These pores are formed due to the oxidation of amino groups during calcination. Among these metal phosphates, cobalt phosphate was further studied which showed good properties like low overpotential, small

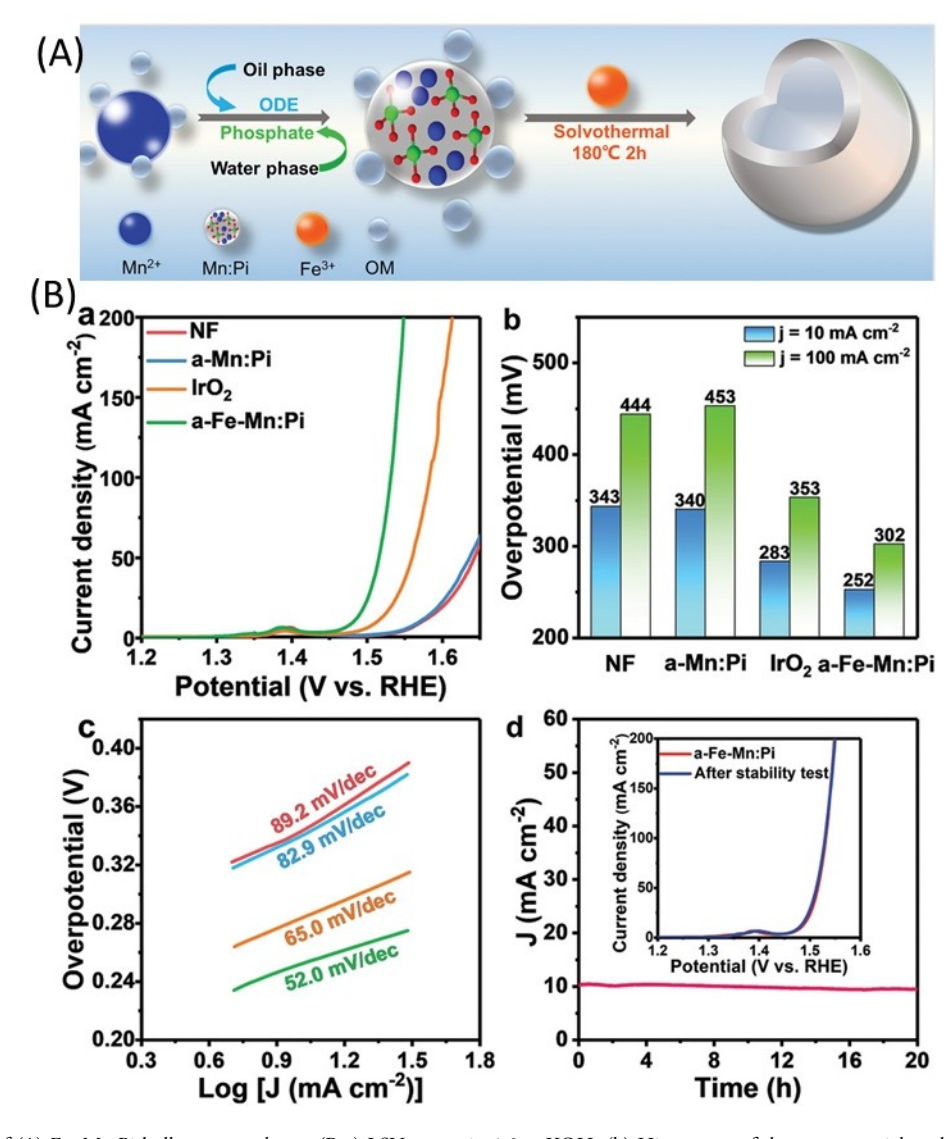


Figure 7. (a) Synthesis of (A) Fe–Mn:Pi hollow nanospheres. (B-a) LSV curves in 1.0 $\,$ m KOH, (b) Histograms of the overpotential at the current density of 10 and 100 mA cm $^{-2}$ from LSV curves,(c) The corresponding Tafel slope plots of Fe–Mn:Pi, Mn:Pi, Ni foam, and IrO₂ and d) Chronoamperometric measurement of the OER at a current density of 10 mA cm $^{-2}$ for a-Fe–Mn:P. Reprinted with permission. [78] Copyright 2020 John Wiley and Sons.

Tafel slope, and excellent stability. These properties showed that N-CoP possesses outstanding oxygen evolution reaction performance. [109]

Metal phosphates are widely used as a catalyst in electrocatalytic reactions like HER and ORR, due to their large radius, isotropic structure, and unsaturated surface area. Metal phosphate/oxide possess high oxidation nature. The oxides can be dissolved by using an acidic medium to create metal phosphate as a true catalytic site for reaction. Moreover, mixed metal phosphate or phosphide are also used due to their long-time stability and well-dispersed form which possesses high HER and ORR performance. N-doped carbon-coated hollow spherical metal phosphate (CoP/Co₂P) was synthesized

by pyrolysis to study the electrocatalysis of water under alkaline conditions. The result showed the highest stability towards HER and OER at an overpotential of 125 mV and 273 mV at a current density of 10 mA cm⁻². Similarly, for ORR the half-wave potential of 0.860 V or higher was obtained which was 36 mV higher as compared to Pt/C.^[111] Heteroatom doped NiP showed greater enhancement towards catalytic activity for HER due to an increase in density of reactive sites as well as regulating the adsorption/desorption capacity of reacting intermediate.^[112]

 $\text{Co(PO_3)_2/MoO_4/rGO}$ metal phosphate was synthesized by anion exchange and phosphating process which was used as a catalyst for water splitting at 1.0 M KOH solution. The

15280961, 2022, 8, Downbaded from https://onlinelbrary.wiley.com/doi/10.1002/trc.202200084 by North Carolina A&T University, Wiley Online Library on [21/07/2023]. See the Terms and Conditions (https://onlinelibrary.wiley.com/terms-and-conditions) on Wiley Online Library for rules of use; OA articles are governed by the applicable Creative Commons. License

overpotential for HER was found to be 140 mV and for OER 290 mV. The stability of samples after long-term use for HER and OER was also higher than Pt/C and IrO2 respectively. [113] Red P deposited on TiO2 hollow sphere was synthesized through the chemical vapor deposition method. When the experiment was performed, the HER was found to be 2.5 times higher than Red P and 11.1 times higher as compared to TiO2. This is due to improved light-harvesting efficiency of a hollow sphere, light absorbance of Red P, and improved charge separation between TiO₂ and Red P interface. [114] Co_vP hollow nanosphere embedded in N-doped carbon nanotubes were prepared for the water-splitting reaction in 1.0 M KOH. The result was found to be the overpotential of 118 mV for HER and 256 mV for OER.[115] Another catalytic study was conducted with hollow nickel phosphates synthesized by the micelles template method resulting from three chemically distinct triblock copolymers. The synthesized Ni-P material was sub-50nm hollow nanospheres, which catalytically converted p-nitrophenol to p-aminophenol. [33] Using ethylene diamine tetra(methylene phosphonic acid), a hierarchically porous shell of hollow manganese phosphate microsphere was synthesized by a template-free hydrothermal method which can be used as a binding site for heavy metal adsorption like Cu²⁺ ions and protein adsorption due to its outstanding size selectivity. These outstanding results explore the application of microspheres in the purification of heavy metals and pollutants from water. [116] The aluminum phenylphosphonate with an anionic core and a cationic shell can adsorb cationic dyes and anionic inorganic complex as shown in Figure 8. [117] The oxidation-reduction capacity of iron (Fe³⁺/Fe²⁺) to metal ions makes the iron phosphate an ideal adsorbent for metal ions. [118,119] Iron phosphate synthesized via co-precipitation

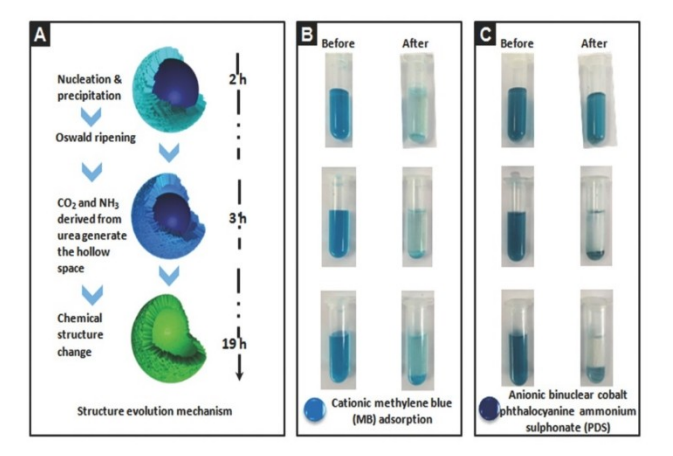


Figure 8. (a) The structure evolution mechanism of aluminum phenylphosphonate microsphere, (b) cationic methylene blue and (c) anionic binuclear cobalt phthalocyanine ammonium sulphonate adsorption using different aluminum phenylphosphonate microsphere.^[117]

method has been used to adsorb uranium from wastewater. [120] The spectroscopic technique reveals that the adsorption is mainly driven by adsorption-reducation mechanism and coordination complex formation between adsorbent and metal ions

4. Conclusion and Future Perspectives

The detailed challenges and synthesis procedures for hollow transition metal phosphates along with their various applications were explored in this review. Precipitation reaction between the metal and phosphate ions, superfluous aggregation, and appropriate phosphate precursors persist as the focal challenges in attaining applicable hollow metal phosphates. Despite the synthetic challenges, hollow nanomaterials retain enthralling structural features of high porosity, low mass density, large surface area, and an increase in the contact area. Therefore, more focus should be drawn to the established synthetic approaches and modified to the production of more hollow metal phosphates with enhanced functionality and diversified applications. Proper template selection allows controlling the void space and shell thickness of hollow particles. Using low molecular weight surfactant supports inducing micro/mesopores on the shell. The through porosity on the shell with hollow voids improves the aforementioned application as the molecules or ions can diffuse in and out of the hollow voids easily. One of the challenges during synthesis is controlling the rapid precipitation reaction between metal ions andphosphate ions. This leads to the formation of unnecessary agglomeration which not only precludes the formation of controlled fine structure but also decreases the surface area. The strategically designed block copolymer could be used to overcome these issues by strongly binding the metal ions and controlling the mineralization of metal phosphate in the polymeric system. The laboratory synthesized stabilizers and templating agents give the targeted structure, as its chemistry can be easily controlled. However, it is expensive and difficult to scale up. The continuous efforts and resourceful investigation show the easy and cost-effective way to synthesize hollow transition metal phosphate. For the applications, the hollow structure should satisfy multiple requirements depending on where they are being used. Biodegradability and biocompatibility are major challenges for bioapplications. Modification or functionalization of metal phosphates can be done to enhance their efficacy.

Acknowledgments

BPB thanks the National Science Foundation Excellence in Research (2100710) USA. Authors thank to Mr. Albert Bastakoti for cover design.

and-conditions) on Wiley Online Library for rules

of use; OA articles are governed by the applicable Creative Commons License

References

- [1] G. J. Hutchings, J. Mater. Chem. 2004, 14, 3385.
- [2] Y. Wang, X. Wang, Z. Su, Q. Guo, Q. Tang, Q. Zhang, H. Wan, Catal. Today 2004, 93–95, 155.
- [3] X. Tian, W. He, J. Cui, X. Zhang, W. Zhou, S. Yan, X. Sun, X. Han, S. Han, Y. Yue, J. Colloid Interface Sci. 2010, 343, 344.
- [4] T.-Y. Ma, X.-J. Zhang, Z.-Y. Yuan, Microporous Mesoporous Mater. 2009, 123, 234.
- [5] R.-K. Chiang, R.-T. Chiang, Inorg. Chem. 2007, 46, 369.
- [6] M. Machida, Chem. Rec. 2016, 16, 2219.
- [7] M. Pramanik, A. Bhaumik, J. Mater. Chem. A 2013, 1, 11210.
- [8] X. S. Li, A. R. Courtney, W. Yantasee, S. V. Mattigod, G. E. Fryxell, *Inorg. Chem. Commun.* **2006**, *9*, 293.
- [9] M. Guan, F. Tao, J. Sun, Z. Xu, Langmuir 2008, 24, 8280.
- [10] Z. Wang, Z. Xu, X. Shi, X. Wang, Q. Zhu, J.-G. Li, Chem. Eng. J. 2018, 343, 16.
- [11] N. F. Dummer, J. K. Bartley, G. J. Hutchings, in *Adv. Catal.*, Elsevier—2011, Vol. 54, pp. 189–247.
- [12] R. Lin, Y. Ding, L. Gong, W. Dong, J. Wang, T. Zhang, J. Catal. 2010, 272, 65.
- [13] G. Li, Z. Hong, H. Yang, D. Li, J. Alloys Compd. 2012, 532, 98
- [14] K. Wang, T. Li, H. Zeng, G. Zou, Q. Zhang, Z. Lin, *Inorg. Chem.* 2018, 57, 8726.
- [15] G. Alberti, F. Marmottini, S. Murcia-Mascarós, R. Vivani, Angew. Chem. Int. Ed. Engl. 1994, 33, 1594.
- [16] X.-J. Zhang, T.-Y. Ma, Z.-Y. Yuan, *Chem. Lett.* **2008**, *37*, 746.
- [17] X. W. (David) Lou, L. A. Archer, Z. Yang, Adv. Mater. 2008, 20, 3987.
- [18] K. An, T. Hyeon, Nano Today 2009, 4, 359.
- [19] J. Hu, M. Chen, X. Fang, L. Wu, Chem. Soc. Rev. 2011, 40, 5472.
- [20] M. Pramanik, R. R. Salunkhe, M. Imura, Y. Yamauchi, ACS Appl. Mater. Interfaces 2016, 8, 9790.
- [21] W. Li, X. Guo, P. Geng, M. Du, Q. Jing, X. Chen, G. Zhang, H. Li, Q. Xu, P. Braunstein, H. Pang, Adv. Mater. 2021, 33, 2105163.
- [22] G. Zhang, Y. Li, X. Xiao, Y. Shan, Y. Bai, H.-G. Xue, H. Pang, Z. Tian, Q. Xu, Nano Lett. 2021, 21, 3016.
- [23] S. Zheng, Q. Li, H. Xue, H. Pang, Q. Xu, Natl. Sci. Rev. 2020, 7, 305.
- [24] H. Zhou, M. Zheng, H. Tang, B. Xu, Y. Tang, H. Pang, Small 2020, 16, 1904252.
- [25] S. Zheng, H. Zhou, H. Xue, P. Braunstein, H. Pang, J. Colloid Interface Sci. 2022, 614, 130.
- [26] M. M. Samy, S. U. Sharma, M. G. Mohamed, A. A. K. Mohammed, S. V. Chaganti, J.-T. Lee, S.-W. Kuo, *Mater. Chem. Phys.* **2022**, 287, 126177.
- [27] M. G. Mohamed, S. V. Chaganti, M.-S. Li, M. M. Samy, S. U. Sharma, J.-T. Lee, M. H. Elsayed, H.-H. Chou, S.-W. Kuo, ACS Appl. Mater. Interfaces 2022, 5, 6442.
- [28] M. G. Mohamed, S. U. Sharma, N.-Y. Liu, T. H. Mansoure, M. M. Samy, S. V. Chaganti, Y.-L. Chang, J.-T. Lee, S.-W. Kuo, *Int. J. Mol. Sci.* 2022, 23, 3174.

- [29] M. G. Mohamed, E. C. Atayde, B. M. Matsagar, J. Na, Y. Yamauchi, K. C.-W. Wu, S.-W. Kuo, J. Inst. Chem. 2020, 112, 180.
- [30] B. Liu, X. Hu, in Advanced Nanomaterials for Pollutant Sensing and Environmental Catalysi— Elsevier, 2020, pp. 1–38.
- [31] Y.-P. Zhu, Y.-L. Liu, T.-Z. Ren, Z.-Y. Yuan, RSC Adv. 2014, 4, 16018.
- [32] P. Półrolniczak, S. Kowalak, J. Porous Mater. 2011, 18, 703.
- [33] B. P. Bastakoti, S. Munkaila, S. Guragain, *Mater. Lett.* **2019**, *251*, 34.
- [34] B. P. Bastakoti, M. Inuoe, S. Yusa, S.-H. Liao, K. C.-W. Wu, K. Nakashima, Y. Yamauchi, *Chem. Commun.* 2012, 48, 6532.
- [35] B. P. Bastakoti, S. Guragain, Y. Yokoyama, S. Yusa, K. Nakashima, *Langmuir* **2011**, *27*, 379.
- [36] O. Olatidoye, D. Thomas, B. P. Bastakoti, New J. Chem. 2021, 45, 15761.
- [37] B. P. Bastakoti, J. Bentley, D. McLaurin, S. Yusa, S. Shaji, N. R. Mucha, D. Kumar, T. Ahamad, J. Mol. Liq. 2020, 305, 112785.
- [38] B. P. Bastakoti, S. Ishihara, S.-Y. Leo, K. Ariga, K. C.-W. Wu, Y. Yamauchi, *Langmuir* 2014, 30, 651.
- [39] W. Zhang, P. Oulego, S. K. Sharma, X.-L. Yang, L.-J. Li, G. Rothenberg, N. R. Shiju, ACS Catal. 2020, 10, 3958.
- [40] J. Feng, Y. Yin, Adv. Mater. 2019, 31, 1802349.
- [41] C. Chen, W. Chen, J. Lu, D. Chu, Z. Huo, Q. Peng, Y. Li, Angew. Chem. 2009, 121, 4910.
- [42] J. Liu, H. Xia, D. Xue, L. Lu, J. Am. Chem. Soc. 2009, 131, 12086.
- [43] E. Mohseni-Vadeghani, R. Karimi-Soflou, A. Karkhaneh, Mater. Lett. 2021, 284, 128972.
- [44] R. Cai, Y. Du, W. Zhang, H. Tan, T. Zeng, X. Huang, H. Yang, C. Chen, H. Liu, J. Zhu, S. Peng, J. Chen, Y. Zhao, H. Wu, Y. Huang, R. Xu, T. M. Lim, Q. Zhang, H. Zhang, Q. Yan, Chem. Eur. J. 2013, 19, 1568.
- [45] Y. Yan, B. Y. Xia, X. Ge, Z. Liu, A. Fisher, X. Wang, Chem. Eur. J. 2015, 21, 18062.
- [46] N. Li, Z. Xu, Y. Liu, Z. Hu, J. Power Sources 2019, 426, 1.
- [47] Z. Xiao, Y. Bao, Z. Li, X. Huai, M. Wang, P. Liu, L. Wang, ACS Appl. Mater. Interfaces 2019, 2, 1086.
- [48] J. Tan, X. Y. Li, F. Yang, J. Liu, Adv. Mater. Res. 2011, 399–401, 625.
- [49] R. Bendi, V. Kumar, V. Bhavanasi, K. Parida, P. S. Lee, *Adv. Energy Mater.* **2016**, *6*, 1501833.
- [50] H. Karimi, Iran. J. Sci. Technol. Trans. Sci. 2018, 42, 219.
- [51] L. Chen, J.-T. Ren, Y.-S. Wang, W.-W. Tian, L.-J. Gao, Z.-Y. Yuan, ACS Sustainable Chem. Eng. 2019, 7, 13559.
- [52] X. Li, J. Tang, G. Wang, Y. Lu, C. Zhang, G. Jia, Solid State Sci. 2020, 107, 106354.
- [53] J. Tian, F. Zhang, Y. Han, X. Zhao, C. Chen, C. Zhang, G. Jia, Appl. Surf. Sci. 2019, 475, 264.
- [54] J.-T. Ren, L. Chen, H.-Y. Wang, Z.-Y. Yuan, Chem. Eng. J. 2021, 418, 129447.
- [55] J.-T. Ren, L. Chen, Y. Liu, Z.-Y. Yuan, J. Mater. Chem. A 2021, 9, 11370.
- [56] C. Cui, X. Lai, R. Guo, E. Ren, W. Qin, L. Liu, M. Zhou, H. Xiao, Electrochim. Acta 2021, 393, 139076.

- [57] H. Tamai, T. Ikeya, F. Nishiyama, H. Yasuda, K. Iida, S. Nojima, J. Mater. Sci. 2000, 35, 4945.
- [58] M.-Q. Wang, C. Ye, S.-J. Bao, M.-W. Xu, Microchim. Acta 2017, 184, 1177.
- [59] J. Xu, D. Xiong, I. Amorim, L. Liu, ACS Appl. Nano Mater. 2018, 1, 617.
- [60] S.-Y. Duan, J.-Y. Piao, T.-Q. Zhang, Y.-G. Sun, X.-C. Liu, A.-M. Cao, L.-J. Wan, NPG Asia Mater. 2017, 9, e414.
- [61] X. Zhang, L. Zhang, G. Xu, A. Zhao, S. Zhang, T. Zhao, J. Colloid Interface Sci. 2020, 561, 23.
- [62] M. Pramanik, C. Li, M. Imura, V. Malgras, Y.-M. Kang, Y. Yamauchi, Small 2016, 12, 1709.
- [63] H. Wen, M. Cao, G. Sun, W. Xu, D. Wang, X. Zhang, C. Hu, J. Phys. Chem. C 2008, 112, 15948.
- [64] J. Xie, M. Gao, M. Wu, X. Guo, W. Xiong, Q. Kong, F. Zhang, J. Zhang, Chem. Lett. 2020, 49, 677.
- [65] R. Murugavel, A. Choudhury, M. G. Walawalkar, R. Pothiraja, C. N. R. Rao, *Chem. Rev.* 2008, 108, 3549.
- [66] N. Dupré, J. Gaubicher, J. Angenault, G. Wallez, M. Quarton, *J—Power Sources* **2001**, *97–98*, 532.
- [67] N. Dupré, J. Gaubicher, T. Le Mercier, G. Wallez, J. Angenault, M. Quarton Solid State Ionics 2001, 140, 209
- [68] W. He, C. Wei, X. Zhang, Y. Wang, Q. Liu, J. Shen, L. Wang, Y. Yue, *Electrochim. Acta* 2016, 219, 682.
- [69] P. L. Mani Kanta, N. L. Priya, P. Oza, M. Venkatesh, S. K. Yadav, B. Das, G. Sundararajan, R. Gopalan, ACS Appl. Mater. Interfaces 2021, 4, 12581.
- [70] X. Zhu, Z. Li, X. Jia, W. Dong, G. Wang, F. Wei, Y. Lu, ACS Sustainable Chem. Eng. 2018, 6, 15608.
- [71] T.-F. Hung, W.-J. Cheng, W.-S. Chang, C.-C. Yang, C.-C. Shen, Y.-L. Kuo, *Chem. Eur. J.* 2016, 22, 10620.
- [72] H. Kim, A. Prasad Tiwari, T. Mukhiya, H. Y. Kim, J. Colloid Interface Sci. 2021, 600, 740.
- [73] A. Clearfield, G. D. Smith, Inorg. Chem. 1969, 8, 431.
- [74] B. Pan, Q. Zhang, W. Du, W. Zhang, B. Pan, Q. Zhang, Z. Xu, Q. Zhang, Water Res. 2007, 41, 3103.
- [75] Y. Feng, W. He, X. Zhang, X. Jia, H. Zhao, *Mater. Lett.* 2007, 61, 3258.
- [76] Y. Zhu, K. Kanamori, N. Moitra, K. Kadono, S. Ohi, N. Shimobayashi, K. Nakanishi, *Microporous Mesoporous Mater.* 2016, 225, 122.
- [77] Z.-Y. Yuan, T.-Z. Ren, A. Azioune, J.-J. Pireaux, B.-L. Su, *Catal. Today* **2005**, *105*, 647.
- [78] Y. Liu, J. Zhang, W. Wang, L. Cao, B. Dong, Adv. Sustainable Syst. 2020, 4, 2000128.
- [79] T. Zhang, S. Zhang, S. Cao, Q. Yao, J. Y. Lee, *Chem. Mater.* 2018, 30, 8270.
- [80] M. Amiri, S. E. Moosavifard, S. S. H. Davarani, S. K. Kaverlavani, M. Shamsipur, *Chem. Eng. J.* 2021, 420, 129910.
- [81] S. Alam, M. Z. Iqbal, Ceram. Int. 2021, 47, 11220.
- [82] C. Chen, N. Zhang, X. Liu, Y. He, H. Wan, B. Liang, R. Ma, A. Pan, V. A. L. Roy, ACS Sustainable Chem. Eng. 2016, 4, 5578
- [83] H. Zhao, Z. Yuan, ChemCatChem 2020, 12, 3797.
- [84] B. P. Bastakoti, Y. Li, S. Guragain, M. Pramanik, S. M. Alshehri, T. Ahamad, Z. Liu, Y. Yamauchi, *Chem. Eur. J.* 2016, 22, 7463.

- [85] S. Tang, X. Huang, X. Chen, N. Zheng, Adv. Funct. Mater. 2010, 20, 2442.
- [86] J. Zhao, Z. Jian, J. Ma, F. Wang, Y.-S. Hu, W. Chen, L. Chen, H. Liu, S. Dai, *ChemSusChem* 2012, 5, 1495.
- [87] L. Wang, J. Li, H. Zhou, Z. Huang, S. Tao, B. Zhai, L. Liu, L. Hu, J. Mater. Sci. Mater. Electron. 2018, 29, 9283.
- [88] Y. Fang, Q. Liu, L. Xiao, X. Ai, H. Yang, Y. Cao, ACS Appl. Mater. Interfaces 2015, 7, 17977.
- [89] M. Wu, W. Ni, J. Hu, J. Ma, Nano-Micro Lett. 2019, 11, 44.
- [90] V. Sharmila, R. Packiaraj, N. Nallamuthu, M. Parthibavarman, *Inorg. Chem. Commun.* 2020, 121, 108194.
- [91] H. Pang, Y.-Z. Zhang, Z. Run, W.-Y. Lai, W. Huang, *Nano Energy* 2015, 17, 339.
- [92] B. Li, P. Gu, Y. Feng, G. Zhang, K. Huang, H. Xue, H. Pang, Adv. Funct. Mater. 2017, 27, 1605784.
- [93] M. Wang, Y. Zhao, X. Zhang, R. Qi, S. Shi, Z. Li, Q. Wang, Y. Zhao, Electrochim. Acta 2018, 272, 184.
- [94] M. Z. Iqbal, J. Khan, S. Siddique, A. M. Afzal, S. Aftab, *Int. J. Hydrogen Energy* 2021, 46, 15807.
- [95] Z. Tang, N. Kong, J. Ouyang, C. Feng, N. Y. Kim, X. Ji, C. Wang, O. C. Farokhzad, H. Zhang, W. Tao, *Matter* 2020, 2, 297
- [96] G. Renaudin, S. Gomes, J.-M. Nedelec, *Materials* 2017, 10, 92.
- [97] H. Luo, D. Gong, F. Yang, R. Zeng, Y. Zhang, L. Tan, *Mater. Express* 2021, 11, 123.
- [98] Z. Wang, G. Li, Y. Gao, Y. Yu, P. Yang, B. Li, X. Wang, J. Liu, K. Chen, J. Liu, W. Wang, *Chem. Eng. J.* 2021, 404, 125574.
- [99] G. Gnanamoorthy, V. K. Yadav, D. Ali, V. Narayanan, K. Mohammed Saleh Katubi, S. Alarifi, Opt. Mater. 2021, 117, 111113.
- [100] X. Yuan, B. Zhu, X. Ma, G. Tong, Y. Su, X. Zhu, *Langmuir* 2013, 29, 12275.
- [101] J. Tian, F. Zhang, C. Zhang, W. Wang, Y. Liu, G. Jia, Colloids Surf. Physicochem. Eng. Asp. 2019, 568, 195.
- [102] H. Hu, P. Zhao, J. Liu, Q. Ke, C. Zhang, Y. Guo, H. Ding, J. Nanobiotechnol. 2018, 16, 98.
- [103] P.-P. Li, Y. Yan, H.-T. Zhang, S. Cui, C.-H. Wang, W. Wei, H.-G. Qian, J.-C. Wang, Q. Zhang, J. Controlled Release 2020, 328, 45.
- [104] J. Yu, R. Hao, F. Sheng, L. Xu, G. Li, Y. Hou, Nano Res. 2012, 5, 679.
- [105] J. V. Rojas, J. D. Woodward, N. Chen, A. J. Rondinone, C. H. Castano, S. Mirzadeh, Nucl. Med. Biol. 2015, 42, 614.
- [106] N. Pethan Rajan, G. S. Rao, V. Pavankumar, K. V. R. Chary, Catal. Sci. Technol. 2014, 4, 81.
- [107] H. Mao, X. Li, F. Xu, Z. Xiao, W. Zhang, T. Meng, Catalysts 2021, 11, 531.
- [108] G. T. Whiting, J. K. Bartley, N. F. Dummer, G. J. Hutchings, S. H. Taylor, *Appl. Catal. A* 2014, 485, 51.
- [109] X. Guo, N. Li, Y. Cheng, G. Wang, Y. Zhang, H. Pang, Chem. Eng. J. 2021, 411, 128544.
- [110] X.-Y. Zhang, W.-L. Yu, J. Zhao, B. Dong, C.-G. Liu, Y.-M. Chai, Appl. Mater. Res. 2021, 22, 100913.
- [111] L. Bo, W. Liu, R. Liu, Y. Hu, L. Pu, F. Nian, Z. Zhang, P. Li, J. Tong, *Electrochim. Acta* 2022, 403, 139643.

- [112] Y. Yu, Q. Chen, J. Li, P. Rao, R. Li, Y. Du, C. Jia, W. Huang, J. Luo, P. Deng, Y. Shen, X. Tian, J. Colloid Interface Sci. 2022, 607, 1091.
- [113] D. Zhao, S. Ning, X. Yu, Q. Wu, W. Zhou, J. Dan, Y. Zhu, H. Zhu, N. Wang, L. Li, J. Colloid Interface Sci. 2022, 609, 269.
- [114] G. Huang, W. Ye, C. Lv, D. S. Butenko, C. Yang, G. Zhang, P. Lu, Y. Xu, S. Zhang, H. Wang, Y. Zhu, D. Yang, *J. Mater. Sci. Technol.* 2022, 108, 18.
- [115] Z. Lu, Y. Cao, J. Xie, J. Hu, K. Wang, D. Jia, Chem. Eng. J. 2022, 430, 132877.
- [116] Y.-P. Zhu, Y.-L. Liu, T.-Z. Ren, Z.-Y. Yuan, Nanoscale 2014, 6, 6627.

- [117] L. Zhang, K. Qian, X. Wang, F. Zhang, X. Shi, Y. Jiang, S. Liu, M. Jaroniec, J. Liu, Adv. Sci. 2016, 3, 1500363.
- [118] R. Li, Q. Li, X. Sun, J. Li, J. Shen, W. Han, L. Wang, J. Hazard. Mater. 2020, 392, 122509.
- [119] R. N. Collins, K. M. Rosso, J. Phys. Chem. A 2017, 121, 6603.
- [120] N. Pan, J. Tang, D. Hou, H. Lei, D. Zhou, J. Ding, Chem. Eng. J. 2021, 423, 130267.

Manuscript received: April 11, 2022 Revised manuscript received: June 3, 2022 Version of record online: July 11, 2022